Measurement of ^{12}C, ^{16}O, and ^{56}Fe charge changing cross sections in helium at high energy, comparison with cross sections in hydrogen, and application to cosmic-ray propagation

P. Ferrando,[a] W. R. Webber,[b] P. Goret,[a] J. C. Kish,[b] D. A. Schrier,[b]
A. Soutoul,[a] and O. Testard,[a]
[a]*Département de Physique Générale Service d'Astrophysique, Centre d'Etudes Nucléaires de Saclay, 91191 Gif-sur-Yvette, Cedex, France*
[b]*Space Science Center, University of New Hampshire, Durham, New Hampshire 03824*
(Received 14 September 1987)

We present measurements of the spallation cross sections of carbon, oxygen, and iron in helium and hydrogen, at beam energies from 540 to 1600 MeV/nucleon, performed by exposing liquid helium, CH_2, and C targets. Charge changing cross sections are reported for fragments down to Ne for Fe+α and Fe+p reactions, and down to B for O+α, O+p, C+α, and C+p reactions. α- to p-induced cross section ratios (σ_α/σ_p) are determined at the same energy per nucleon. From these measurements an empirical formula for the σ_α/σ_p ratios is derived, and is found in good agreement with available isotopic cross sections data from radioactivity and radiochemical techniques. These results are applied to the propagation of heavy charged cosmic rays in an interstellar medium with an helium to hydrogen abundance ratio of 0.10. It is shown that the Sc–Mn/Fe ratio prediction is decreased relative to the B/C ratio when compared to propagation calculations in a pure hydrogen interstellar medium.

I. INTRODUCTION

In recent years considerable progress has been achieved in the measurement of cosmic-ray elemental ratios (e.g., Ref. 1) and in the determination of the cross sections for p-induced reactions, especially by the New Hamsphire group (e.g., Ref. 2). This progress paved the way to an accurate investigation of the cosmic-ray propagation through the galaxy. In particular, using cross sections that were available in 1985, it was found that the most simple model of propagation (the leaky-box model[3]), with a constant probability per unit time for cosmic rays to escape the galaxy, encounters some difficulty in reconciling the observed B/C and Sc–Mn (Sc + Ti + V + Cr + Mn)/Fe ratios, Sc–Mn/Fe being underpredicted when compared to B/C.[4–6] However, it is a feature common of all propagation calculations either to neglect the spallation of cosmic rays with interstellar helium, or to assume a simple scaling of α-induced to p-induced reactions cross sections, an assumption that leads to no differential effect between the B/C and Sc–Mn/Fe ratios. Since interstellar helium is actually responsible for $\sim$20% of the spallations of cosmic rays, one may wonder if the difficulty mentioned above is not due to the neglect of interstellar helium. In a preliminary analysis, Ferrando *et al.*[7] have suggested that a careful introduction of the α-induced cross sections in propagation calculations should, in fact, increase the underprediction of Sc–Mn/Fe when B/C is accounted for in the leaky-box model. This conclusion relied on a few spallation data only, and called for a more detailed study. Unfortunately, available measurements of α-induced cross sections, reviewed by Read and Viola[8] for spallation of light nuclei, are quite scarce and restricted to very low energy, except for the production of a handful of radioactive isotopes from C, O, Fe, and Ni nuclei.[9,10]

We have therefore initiated a series of measurements of α-particle reactions cross sections; the first results concerning C, O, and Fe spallation are presented in this paper. The measurements were performed with high energy beams, provided by the Lawrence Berkeley Laboratory BEVALAC, impinging on a specially designed liquid helium target placed in front of the New Hampshire group telescope. Under the same conditions the cross sections in hydrogen were also measured, allowing for meaningful comparisons between cross sections for α- and p-induced reactions. Results concerning isotopic cross sections in helium, not yet fully analyzed, will be reported later.

The experimental details and the data analysis procedure are given in Secs. II and III, respectively. Section IV first presents the systematics of the cross sections for α-induced reactions compared to p-induced reactions, and then discusses the factorization hypothesis of Fe fragmentation cross sections. A simple empirical formula for the ratio of α-induced to p-induced cross sections at the same energy per nucleon is proposed in Sec. V. Finally, Sec. VI investigates the influence of interstellar helium on the propagation of cosmic rays, focusing on the B/C vs Sc–Mn/Fe problem.

II. EXPERIMENTAL DETAILS

The telescope, shown in Fig. 1, is very similar to that already used on numerous occasions to measure spallation cross sections in CH_2 and C by the New Hampshire group.[11–13] The results reported in this paper are from

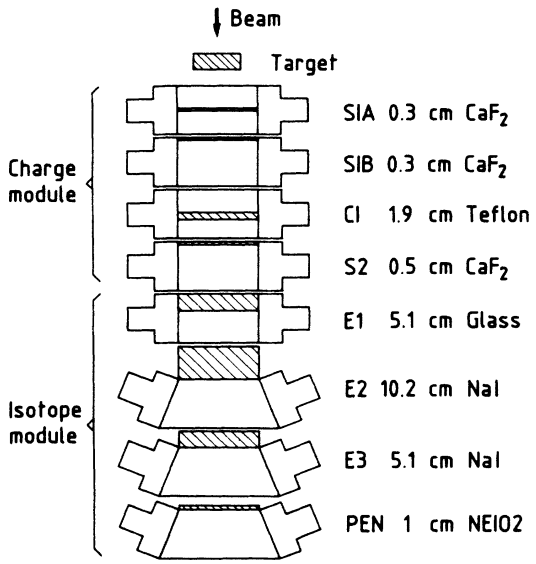

FIG. 1. Sketch of the telescope.

the charge identification module only, which consists of two CaF_2 scintillators, a glass Čerenkov detector, and a third CaF_2 scintillator. In front of this telescope were placed the different targets. The final element in the charge module defines the acceptance cone with half-angle θ about the beam axis. For the ^4He target θ increases from 3.6° to 5.8° from one end of the target to the other; for CH_2 and C targets θ is $\sim 7.7°$. These large acceptance angles ensure that almost all fragments considered in this work ($Z > 4$) are detected in the telescope. To be more specific, let us consider the worst case, i.e., $\theta = 3.6°$ and B nuclei at 600 MeV/nucleon. The maximum transverse momentum p_t for B nuclei to be detected is 470 MeV/c, i.e., 2.7 times the standard deviation of the p_t Gaussian distribution,[14–16] indicating that less than 0.7% of the B fragments are out of the detector geometry.

The helium target is shown in Fig. 2. It was designed in order to present a reasonable interaction length to C and O beams, and to ensure a constant thickness during the runs. This last point requires the helium bath to be subcooled in order to avoid the presence of bubbles in the liquid. This is achieved through the thermocontrol of the target bath (400 mm long cylinder, diameter 70 mm) by a second liquid helium bath (the thermostat) surrounding the target, except on its titanium windows. The large surface of thermal contact between the target and the thermostat ensures that both are always at the same temperature ($\Delta T < 10^{-2}$ K). The four titanium windows' total thickness is 400 μm (0.18 g/cm^2). The thermal radiation shields, of which there are only six facing the windows, are pure aluminum, with a total thickness of 54 μm (0.015 g/cm^2). From a run with an empty target it was checked that beam interactions in the windows and in the radiation shields are at a level of less than $\sim 1\%$ of the interactions in the liquid helium itself. The thermostat was maintained at ~ 3 K through the monitoring of its pressure during the runs, except for

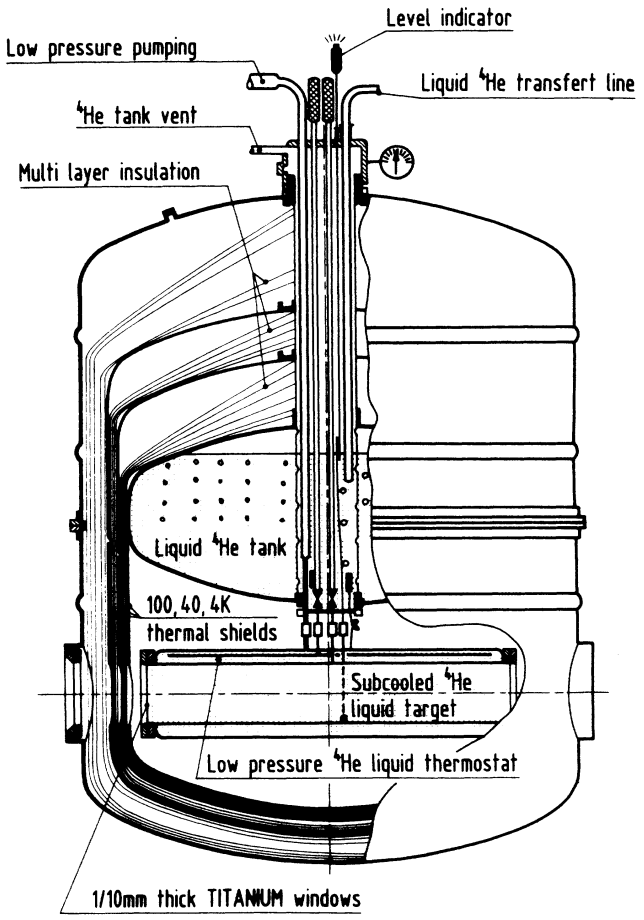

FIG. 2. Sketch of the liquid helium target.

the oxygen runs, for which the manometer was not settled.

For each beam energy, CH_2, C, and ^4He targets were alternated with no target. No target data typically show $< 5\%$ interactions along the beam line and the ~ 2.5 m of air in front of the targets. In Table I are given the pertinent parameters for the different runs, including the interaction lengths obtained for the beam nuclei (Λ_{int}) and the energy in the middle of the targets (E_t). Note that the ^4He target thickness for the oxygen run, not measured, has been estimated to lie between a low and a high value bracketing the measured thicknesses for the other runs, since the operating of the target was similar for all the runs.

III. DATA ANALYSIS

The analysis procedures to obtain the relative abundance of the various charged fragments are similar to that described previously by Webber and Brautigam.[11] Consistency criteria are placed on the outputs of the three CaF_2 counters, and charge histograms of the fragments penetrating the charge module of the telescope are constructed (Fig. 3). The relative abundances obtained from these histograms are first corrected for the no-target background, which is directly subtracted, and

TABLE I. Data for BEVALAC runs. The ^{4}He thickness for the oxygen run was not measured, but is estimated to lie within the quoted interval.

Beam nuclei	Target	Target thickness (g/cm^2)	E_b (MeV/nucleon)	E_t (MeV/nucleon)	Number of events ($\times$1000)	Λ_{int} (g/cm^2)	Total cross section (mb)
C	He	5.66	610	588	307.2	17.0	391±6
		5.60	950	928	682.3	15.7	423±5
		5.64	1600	1580	460.5	15.3	433±5
	CH_2	10.3	610	561	455.5	20.7	1121±9
		8.10	950	915	337.7	19.9	1170±12
		8.31	1600	1572	450.6	19.2	1210±10
	C	12.7	610	561	480.2	28.6	696±6
		10.0	950	915	386.0	27.4	727±8
		10.0	1600	1572	475.3	27.3	730±7
O	He	5.5–5.8	640	612	298.4	13.0	510±20
		5.5–5.8	1600	1573	374.4	13.0	511±20
	CH_2	8.75	640	591	224.3	16.3	1426±14
		8.75	1600	1563	460.3	16.1	1444±10
	C	10.0	640	591	217.6	23.1	861±11
		10.0	1600	1563	443.0	23.1	863±7
Fe	He	5.58	540	434	425.3	6.04	1100±7
		5.64	810	726	523.7	5.90	1126±10
		5.76	1600	1513	628.0	5.54	1199±7
	CH_2	4.84	540	439	330.0	7.95	2924±23
		6.02	810	724	486.2	7.85	2968±16
		6.02	1600	1511	556.1	7.60	3059±16
	C	5.70	540	439	337.5	12.1	1641±15
		7.03	810	724	486.0	12.2	1626±11
		7.03	1600	1511	522.8	11.9	1648±10

then extrapolated to the top of telescope ing semiempirical total cross sections to deterr the amount of interactions suffered by the fragmen in th telescope. The number of noninteracting primary nu ei is obtained from the charge distribution in the first

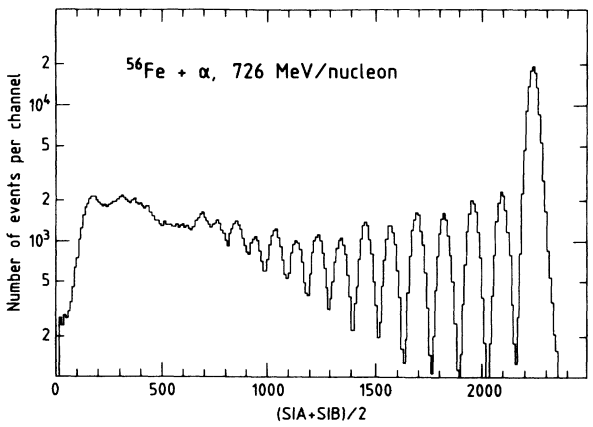

FIG. 3. Charge distribution for $^{56}Fe + \alpha$ reactions at 726 MeV/nucleon, obtained from the average pulse heights of S1A and S1B counters, after data selection.

counter only, which also provides the relative number of secondaries, N_z/N_{tot}. The sum of the corrected individual secondary charge fractions is finally adjusted to equal N_z/N_{tot}, in order to account for the rejection of valid events by the consistency criteria. Corrected relative numbers of events coming out of the helium target are given in Table II.

The total charge changing cross section σ_P of beam nucleus (or primary nucleus) is readily obtained from the primary fraction f_P out of the target, with $\sigma_P = -(m/X)\ln(f_P)$, m being the mass of the target nucleus and X the target thickness. The partial charge changing cross sections $\sigma(P,i)$, for the primary P to fragment into element i, are obtained by solving the set of one-dimensional equations describing the propagation of beam and fragment nuclei through the target:

$$dN_i(x)/dx = -\sigma_i N_i(x)/m + \sum_j \sigma(j,i)N_j(x)/m \ , \qquad (1)$$

$N_i(x)$ being the abundance of the ith element at target depth x, σ_i the total charge changing cross section of element i, and $\sigma(j,i)$ the partial cross section for element j to fragment into element i. For the set of equations (1) to have a unique solution for the $\sigma(P,i)$ we are looking

TABLE II. Elemental abundances out of the helium target for iron, oxygen, and carbon beams. "tot" stands for total number of events.

Ratio	1513 (MeV/nucleon)	726 (MeV/nucleon)	434 (MeV/nucleon)
Fe/tot	0.3538	0.3845	0.3970
Mn/Fe	0.1133	0.1164	0.1274
Cr/Fe	0.0903	0.1012	0.1115
V/Fe	0.0682	0.0774	0.0919
Ti/Fe	0.0706	0.0799	0.0964
Sc/Fe	0.0595	0.0645	0.0789
Ca/Fe	0.0629	0.0724	0.0866
K/Fe	0.0522	0.0565	0.0614
Ar/Fe	0.0560	0.0611	0.0650
Cl/Fe	0.0495	0.0506	0.0527
S/Fe	0.0559	0.0631	0.0628
P/Fe	0.0463	0.0436	0.0476
Si/Fe	0.0724	0.0681	0.0697
Al/Fe	0.0537	0.0498	
Mg/Fe	0.0623	0.0650	
Na/Fe	0.0498		
Ne/Fe	0.0525		

Ratio	1573 (MeV/nucleon)	612 (MeV/nucleon)
O/tot	0.6480	0.6484
N/O	0.0687	0.0770
C/O	0.0812	0.0896
B/O	0.0387	0.0441

Ratio	1580 (MeV/nucleon)	928 (MeV/nucleon)	588 (MeV/nucleon)
C/tot	0.6925	0.7002	0.7168
B/C	0.0563	0.0607	0.0645

for, both total and partial cross sections describing nonprimary fragmentation are specified using assumptions described below.

Total cross sections are computed using a Bradt-Peters-type[17] law

$$\sigma_i = \pi r_0^2 (A_t^{1/3} + A_i^{1/3} - b)^2 , \quad (2)$$

A_t and A_i being the masses of the target and element i nucleus, respectively. For each element, an average mass A_i is chosen according to its various isotopes. b is taken equal to 0.83 as derived for heavy targets,[18] and r_0 is determined from the measured total cross sections.

The choice of partial cross sections for secondaries fragmentation [$\sigma(i,j)$, with $i \neq P$] is less straightforward, and several approaches have been used in the past.[11,18] Here it is assumed that partial cross sections follow the exponential dependence found for p-induced cross sections:[19]

$$\sigma(i,j) = \sigma_0(j) \exp[-(Z_i - Z_j)/\Delta_j] , \quad (3)$$

Z_i, Z_j being the charge of elements i and j, respectively, and Δ_j and $\sigma_0(j)$ being functions of the fragment j only. Then, setting the values of $\sigma(i,j)$ for $\Delta Z = Z_i - Z_j = 1$ reduces the number of unknown cross sections in (1) to the number of $\sigma(P,i)$ to be determined. The $\sigma(i,j)$ for $\Delta Z = 1$ are set in order to be enhanced by the same factor $\Gamma_{\Delta Z=1}$ for all nuclei i when referred to p-induced cross sections. $\Gamma_{\Delta Z=1}$ is obtained from the cross section for the primary nucleus to fragment in the first secondary charge, derived from the data without any assumption. The reference $\Delta Z = 1$ p-induced cross sections are taken from the semiempirical formula recently proposed by Webber.[19]

Finally, we stress that the impact upon partial cross sections of the above assumptions increases with the considered charge change ΔZ, being zero for $\Delta Z = 1$. This is illustrated by the fraction f of detected nuclei of a given charge produced by multiple interactions through the target. For Fe + α reactions at high energy, given the target thickness and the derived cross sections, we find that f is 23% for Sc, while it is 45% for Ne. In the case of O+α reactions, multiple interactions through the target are almost negligible, because of the low ΔZ considered and the longer interaction length ($f = 8\%$ for B).

IV. RESULTS AND SYSTEMATICS

Hereafter, charge changing cross sections in H, He, C, and CH_2 are referred as σ_p, σ_α, σ_C, and σ_{CH_2}, respectively. The results concerning the derived σ_p and σ_α are given in Tables III–V. p-induced cross sections were obtained from those in CH_2 and C with $\sigma_p = (\sigma_{CH_2} - \sigma_C)/2$, and uncertainties upon σ_p from the quadratic sum of uncertainties upon σ_{CH_2} and σ_C. Quoted uncertainties are computed as the quadratic sum of (i) 2 times the statistical uncertainty, and (ii) the uncertainty upon multiple interactions in the target, estimated assuming 20% uncorrelated errors upon the partial cross sections for secondary interactions in the case of the C and CH_2 targets, and 50% in the case of the ^4He target. For O+α runs, the systematic uncertainty due to the target thickness uncertainty was also added.

Considering the σ_α measured in this experiment, only the ^{12}C total cross section can be compared to a previous determination, namely 527±26 mb for the ^{12}C mass changing total σ_α at 0.87 GeV/nucleon by Jaros *et al.*[20] From the ^{12}C charge changing total σ_α of 423±5 mb measured at 0.93 GeV/nucleon, and correcting for ^{11}C production ($\sigma[^{12}C(\alpha,x)^{11}C] = 42 \pm 2$ mb at 700 MeV/nucleon (Ref. 21)), we derive a ^{12}C mass changing total σ_α of 465±6 mb, lower by 12±5% than the value reported by Jaros *et al.*[20] The neglect of ^{10}C production we have made certainly cannot account for this slight discrepancy, since $\sigma[^{12}C(\alpha,x)^{10}C]$ is expected to be less than ~5% of $\sigma[^{12}C(\alpha,x)^{11}C]$ if these two cross sections scale from cross sections in hydrogen by about the same factor.

A. Comparison of α and p reactions

The ratios of α-induced to p-induced cross sections at the same energy per nucleon (i.e., $v_\alpha = v_p$) are given in

TABLE III. Charge changing cross sections for $^{56}Fe+\alpha$ and ^{56}Fe + p reactions, and derived ratios.

	σ_α (mb)	σ_p (mb)	σ_α/σ_p
	1513 MeV/nucleon	1511 MeV/nucleon	
Fe→Mn	129.4±2.4	109.8±2.8	1.18±0.04
Fe→Cr	94.5±4.4	84.4±3.1	1.12±0.07
Fe→V	66.0±4.0	63.7±2.9	1.04±0.08
Fe→Ti	63.4±4.3	62.0±2.8	1.02±0.08
Fe→Sc	49.6±3.9	46.1±2.6	1.08±0.10
Fe→Ca	48.0±4.3	45.9±2.4	1.05±0.11
Fe→K	39.8±3.2	33.2±2.2	1.20±0.12
Fe→Ar	38.8±3.7	33.0±2.1	1.18±0.13
Fe→Cl	31.6±3.4	23.5±1.9	1.34±0.18
Fe→S	35.0±3.4	28.9±1.8	1.21±0.14
Fe→P	25.7±3.1	17.6±1.7	1.46±0.23
Fe→Si	44.7±3.7	25.9±1.7	1.73±0.18
Fe→Al	30.0±3.0	15.0±1.6	2.00±0.29
Fe→Mg	32.1±3.5	14.2±1.5	2.26±0.34
Fe→Na	25.3±2.7	9.5±1.4	2.66±0.48
Fe→Ne	26.8±2.6	9.3±1.4	2.88±0.52
Total σ	1199 ±7	705 ±10	1.70±0.03
	726 MeV/nucleon	724 MeV/nucleon	
Fe→Mn	135.9±2.7	123.2±3.1	1.10±0.04
Fe→Cr	109.1±4.8	98.0±3.6	1.11±0.06
Fe→V	77.1±4.5	73.8±3.5	1.05±0.08
Fe→Ti	73.9±5.0	73.8±3.4	1.00±0.08
Fe→Sc	55.3±4.4	55.9±3.2	0.99±0.10
Fe→Ca	57.5±5.0	52.5±3.0	1.10±0.11
Fe→K	44.4±3.6	30.2±2.6	1.47±0.17
Fe→Ar	42.1±4.4	27.2±2.4	1.55±0.21
Fe→Cl	33.1±3.5	17.6±2.1	1.88±0.30
Fe→S	39.9±4.1	20.5±2.0	1.95±0.28
Fe→P	24.4±3.0	10.8±1.7	2.26±0.45
Fe→Si	40.6±4.0	14.9±1.7	2.72±0.41
Fe→Al	28.9±2.9		
Fe→Mg	36.8±3.7		
Total σ	1126±10	671±10	1.68±0.03
	434 MeV/nucleon	439 MeV/nucleon	
Fe→Mn	150.3±2.8	130.2±4.0	1.15±0.04
Fe→Cr	120.9±5.3	120.3±4.4	1.00±0.06
Fe→V	92.5±5.2	89.9±4.5	1.03±0.08
Fe→Ti	89.7±6.0	84.9±4.2	1.06±0.09
Fe→Sc	67.8±5.4	53.2±3.7	1.27±0.13
Fe→Ca	68.3±6.1	43.8±3.4	1.56±0.18
Fe→K	47.0±4.0	21.3±2.9	2.21±0.35
Fe→Ar	42.9±4.9	19.6±2.6	2.19±0.38
Fe→Cl	33.2±3.8	6.8±2.1	4.88±1.61
Fe→S	37.6±4.3	8.0±2.1	4.70±1.35
Fe→P	26.7±3.3	4.0±1.7	6.68±2.95
Fe→Si	40.1±4.2	6.9±1.8	5.81±1.63
Total σ	1100±7	641±14	1.72±0.04

Tables III–V. Focusing first on total cross sections, the σ_α/σ_p ratios for C, O, and Fe show no important energy dependence within uncertainties, being, on the average, 1.85±0.03 for C, 1.78±0.06 for O, and 1.70±0.02 for Fe. The observed small mass dependence of the σ_α/σ_p ratio looks reasonable on the base of geometric considerations, since, due to their smaller radii, C and O nuclei are more sensitive to the target nucleus radius than the Fe nuclei.

The σ_α/σ_p ratios for partial cross sections do not exhibit such simple features as total cross sections do. They are seen to vary with the energy, the primary nu-

TABLE IV. Same as Table III, for $^{16}O + \alpha$ and ^{16}O + p reactions.

	σ_α (mb)	σ_p (mb)	σ_α/σ_p
	1573 MeV/nucleon	1563 MeV/nucleon	
O→N	80.3±3.7	67.8 ±1.9	1.18±0.06
O→C	89.5±4.7	69.5 ±2.2	1.29±0.08
O→B	40.1±2.8	27.2 ±2.2	1.47±0.16
Total σ	511±20	290±6	1.76±0.08
	612 MeV/nucleon	591 MeV/nucleon	
O→N	90.0±4.4	74.5 ±2.9	1.21±0.07
O→C	98.3±5.6	70.0 ±3.3	1.40±0.10
O→B	45.4±3.4	28.3 ±3.0	1.60±0.21
Total σ	510±20	282 ±9	1.81±0.09

cleus, and the fragment considered. However, the first important trend shown by these data is that the σ_α/σ_p ratio of partial cross sections for a given fragment is generally smaller than the σ_α/σ_p ratio of total cross sections of the beam nucleus producing that fragment. This is always the case for fragments with astrophysical interest, i.e., B from C and O fragmentation, and Sc to Mn from Fe fragmentation. The implication of this regarding cosmic-rays propagation will be discussed in Sec. VI. In the following, we examine in more detail the systematics of the σ_α/σ_p ratios, beginning with Fe fragmentation.

The charge change dependence of the measured σ_α/σ_p ratios for Fe are displayed on the left-hand side of Fig. 4 for three energies. For fragments in the ~Sc–Mn group corresponding to peripheral reactions, the ratios σ_α/σ_p are almost independent of the energy, being always in the ~1.0–1.2 range. On the contrary, for fragments with lower charge the ratio σ_α/σ_p strongly increases as the energy decreases, and may be significantly larger than the ratio for the total cross sections. As seen from the tables, this increase of σ_α/σ_p with energy is, in fact, mainly due to a strong reduction of the p-induced cross sections, the α-induced cross sections showing comparatively negligible variations with energy. As an extreme example, the Fe(p,x)Si cross section decreases by a factor of ~4 from 1511 to 439 MeV/nucleon, while the Fe(α,x)Si cross section only decreases by 10% for the same energy variation. These results are qualitatively similar to those obtained by Raisbeck and Yiou[10] concerning the production of radioactive isotopes from ^7Be to ^{54}Mn in Fe + α and Fe + p reactions at 700 and 1150 MeV/nucleon. These authors have reported isotopic cross sections ratios σ_α/σ_p of 1.0–1.2 for secondaries with $\Delta Z < 6$, and ~4 at 1150 MeV/nucleon for ^{22}Na production, values quite comparable to ratios of charge changing cross sections measured in this work.

Turning now to O and C fragmentation (Tables IV and V, Fig. 5), the σ_α/σ_p ratios for partial cross sections show a systematic similar to that present in Fe reactions involving intermediate charge changes. However, the σ_α/σ_p ratios measured for C and O reactions (particularly into B) is larger than 1, in contrast to that for Fe fragmentation into ~Sc–Mn, where the ratio is ~1 at all energies. Finally, although isotopic cross sections ratios may not be directly comparable to charge changing cross section ratios, we note that the σ_α/σ_p ratios for O spallation determined here are in qualitative agreement with $\sigma_\alpha/\sigma_p = 1.35 \pm 0.4$ for O→^{13}N, and for $\sigma_\alpha/\sigma_p = 1.85 \pm 0.4$ for O→^{11}C measured at a much lower energy[22] (230 MeV/nucleon).

TABLE V. Same as Table III, for $^{12}C + \alpha$ and ^{12}C + p reactions.

	σ_α (mb)	σ_p (mb)	σ_α/σ_p
	1580 MeV/nucleon	1572 MeV/nucleon	
C→B	65.6 ±1.2	53.0 ±1.6	1.24±0.04
Total σ	433 ±5	240±6	1.80±0.05
	928 MeV/nucleon	915 MeV/nucleon	
C→B	71.2 ±1.1	53.1 ±1.9	1.34±0.05
Total σ	423 ±5	221±7	1.91±0.07
	588 MeV/nucleon	561 MeV/nucleon	
C→B	74.9 ±1.6	53.3 ±1.6	1.41±0.05
Total σ	391 ±5	213 ±5	1.84±0.05

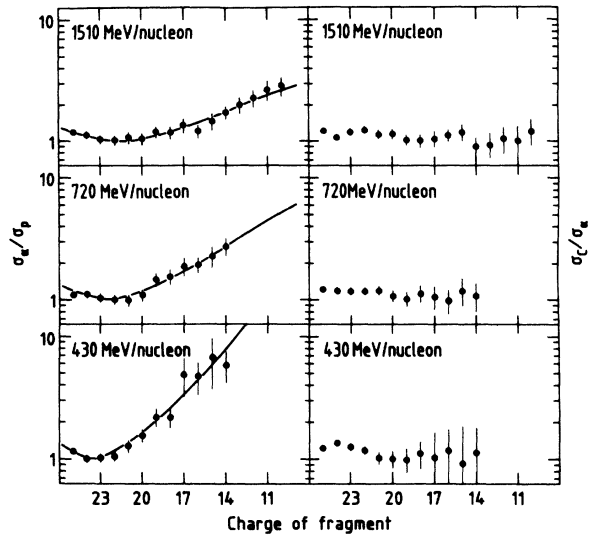

FIG. 4. Ratios of the Fe charge changing cross sections in α and H targets (left), and in C and α targets (right), as a function of the charge of the fragment. The solid lines (left) are from the empirical formula discussed in the text.

B. Implications for factorization of Fe fragmentation cross sections

From the study of Fe fragmentation at 1.9 GeV/nucleon in targets with various masses (from H to U), Westfall *et al.*[18] have suggested that charge changing cross sections could be factored into a target factor, γ_t, depending on the target only, and a fragment factor depending on the considered fragment only. From the results for α- and p-induced reactions reported here, it is clear that such a simple factorization hypothesis does not hold when charge changing cross sections for α- and p-induced reactions are compared. This is especially true at low energy where σ_α/σ_p ratios show a strong dependence with the considered fragment, but also at high energy where this dependence is still present, albeit less.

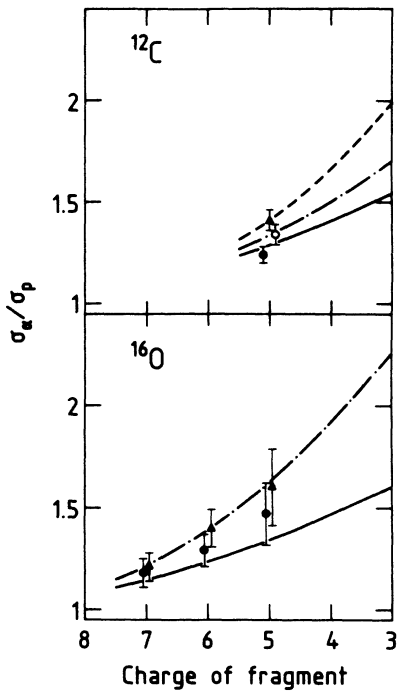

FIG. 5. Same than Fig. 4 for O and C charge changing cross sections at different energies: 1580, 928, and 588 MeV/nucleon (^{12}C), 1573 and 512 MeV/nucleon (^{16}O). Results from the empirical formula are shown as solid lines at 1580 MeV/nucleon (^{12}C) and 1570 MeV/nucleon (^{16}O), dashed-dotted lines at 928 MeV/nucleon (^{12}C) and 612 MeV/nucleon (^{16}O), and a dotted line at 588 MeV/nucleon (^{12}C).

It has already been pointed out that factorization does not apply when cross sections for p-induced and C-induced reactions are compared;[11] however, it appears interesting to look for factorization in the ratios of cross sections for Fe + α and Fe + C reactions, where protons are not involved. These data for Fe are displayed on the right-hand side of Fig. 4. It is seen that the σ_C/σ_α ratios are now rather independent of both the energy and the fragment considered, having average values of 1.12, 1.13, and 1.11 (± 0.03) at 430, 720, and 1510 MeV/nucleon, and showing variations by no more than $\sim 10\%$ from the average over the whole charge range. This supports the hypothesis of factorization of Fe cross sections in heavy targets extending down to helium, at least down to fragment charges of ~ 10. To compare with the target factors γ_t quoted by Westfall *et al.*,[18] we have derived γ_α for the helium target, $\gamma_\alpha = \gamma_C \sigma_\alpha/\sigma_C$, under the same conditions used by these authors, i.e., assuming $\gamma_C = 1.92$, considering only the $Z = 18-24$ fragments and the highest energy data. A value of 1.70 ± 0.06 is obtained for γ_α, which compares well with both analytical target factor dependencies proposed by Westfall *et al.* that result in $\gamma_\alpha = 1.64 \pm 0.15$ and 1.63 ± 0.09. However, the σ_C/σ_α ratio of Fe total cross sections is 1.49, 1.44, and 1.37 (± 0.02) at 430, 720, and 1510 MeV/nucleon, respectively, values significantly larger than $\sigma_\alpha/\sigma_p \sim 1.12$ derived above for spallation cross sections into fragments with charge higher than ~ 10. This indicates that, even for these reactions, factorization certainly breaks down for reactions involving fragment charges lower than ~ 10. We therefore conclude that Fe fragmentation cross sections can be factored into a target and a fragment factor, but only within a limited fragment charge range, and for targets heavier than helium. Although this work tends to show that this limited fragmentation may apply down to 430 MeV/nucleon, it should be kept in mind that the results of Westfall *et al.*[18] were derived at 1.9 GeV/nucleon, and that factorization may not apply at lower energies for targets heavier than C.

V. AN EMPIRICAL FORMULA FOR THE σ_α/σ_p RATIOS

The measurements presented above already constitute an important step for the incorporation of interstellar ^4He in cosmic-ray propagation models, since the cross sections for fragmentation of C, O, and Fe are the most important parameters in determining the amount of matter encountered by cosmic rays. However, with the

aim of including a set of cross sections for α-particle reactions as complete as possible in propagation calculations, it appears useful to provide an analytical fit to the measured σ_α/σ_p ratios that allows a simple extrapolation of these measurements to nuclei intermediate between C, O, and Fe, and to all energies greater than $\sim$200 MeV/nucleon, the natural lower energy limit considered in cosmic-ray propagation because of the solar modulation (except if cosmic rays are reaccelerated during propagation, a problem still in debate). We stress that the empirical formulas for σ_α/σ_p proposed below are certainly not unique, but they were chosen because of their simplicity and their ability to reproduce not only our data, on which they are based, but also the few other available σ_α/σ_p isotopic cross section ratios, especially that involving intermediate nuclei between O and Fe, namely Mg, Al, and Si.

First, for ratios of total cross sections, the following formulation was found suitable:

$$\sigma_\alpha^{\rm tot}/\sigma_p^{\rm tot}(A_i)=a A_i^{-\delta} , \tag{4}$$

with $a=2.10\pm0.10$ and $\delta=0.055\pm0.013$ as derived from our measurements.

Considering now partial cross sections, the σ_α/σ_p ratios for Fe fragmentation runs provide the most complete data set since they clearly show the dependence with energy and with charge change. We first focus on them. Figure 4 suggest a functional form involving ΔZ, the charge difference between beam and fragment charge:

$$\sigma_\alpha/\sigma_p(Z_i,Z_f,E)=\exp(\mu\,|\,\Delta Z-\delta\,|^{\nu}) , \tag{5}$$

Z_i and Z_f being the charge of the beam and fragment nuclei, respectively. The quantity δ represents an offset and accounts for the location of the minimum of the σ_α/σ_p ratio (energy dependent, see Fig. 4). From multiparameter fits of μ, ν, and δ over the whole fragment charge range, it was found that ν can be taken constant as a function of energy, with $\nu=1.43$. Best fit values of μ and δ are, then, for iron fragmentation,

$$\begin{aligned}&\mu=0.031,\quad \delta=4.40 \quad \text{at } 1.51 \text{ GeV/nucleon} ,\\ &\mu=0.047,\quad \delta=3.45 \quad \text{at } 0.73 \text{ GeV/nucleon} ,\\ &\mu=0.082,\quad \delta=2.45 \quad \text{at } 0.43 \text{ GeV/nucleon} .\end{aligned} \tag{6}$$

From χ^2 tests, μ determination is found to be accurate within $\sim$30%, δ determination within $\sim$7%. The fits to the Fe data with expression (5) are shown as solid lines on the left-hand side of Fig. 4.

Turning now to the fit of σ_α/σ_p for O and C beam particles, using the same functional form as in (5), the observation that the σ_α/σ_p are always >1 suggests that the δ parameter should be a negative value when C and O are considered. So, δ is parametrized as a function of the beam charge Z_i:

$$\delta(Z_i,E)=f(Z_i)\delta_{\rm Fe}(E) . \tag{7}$$

Reasonable fits to σ_α/σ_p for C and O cross sections are obtained, as shown in Fig. 5, if ν is kept equal to 1.43, and μ and $\delta_{\rm Fe}(E)$ are linearly interpolated as a function of energy from those used for Fe as given in (6). The following $f(Z_i)$ values are then derived from the data:

$$\begin{aligned}&f(Z_i=6)=-0.76,\quad f(Z_i=8)=-0.41 ,\\ &f(Z_i=26)=+1.00 \text{ by definition} .\end{aligned} \tag{8}$$

The complete expression (5) can then be written in the form showing the dependencies on the primary nuclei charge Z_i and the energy E:

$$\sigma_\alpha/\sigma_p(Z_i,Z_f,E)=\exp[\,\mu(E)\,|\,(Z_i-Z_f)-f(Z_i)\delta_{\rm Fe}(E)\,|^{1.43}] , \tag{9}$$

with $\mu(E)$ and $\delta_{\rm Fe}(E)$ linearly interpolated as a function of E from the values given in (6), and $f(Z_i)$ linearly interpolated as a function of Z_i from the values given in (8). Two precautions must be taken for application of this empirical fit. They are discussed below.

First, since cross sections reach asymptotic values at high energy, $\mu(E)$ and $\delta_{\rm Fe}(E)$ must also reach asymptotic values. For propagation purposes, and in the absence of any other data, we will consider in the next section that these asymptotic values are reached at 1.5 GeV/nucleon, the highest energy in our data.

Second, it must be kept in mind that the exponential dependence in (9) is established on the base of fragmentation cross sections down to $\sim$Ne fragments only. At the present time, it is not possible to correctly assess the fragment charge dependence for very large ΔZ, σ_α/σ_p possibly reaching some asymptotic value or continuing to increase with ΔZ. Actually, if it is assumed that σ_α/σ_p ratios are equal for charge changing cross sections and isotopic cross sections, an exponential increase of σ_α/σ_p over the whole ΔZ range is found to be excessive by a factor of $\sim$2 in view of the radioactive data for Fe$\rightarrow^7$Be at 1.15 GeV/nucleon.[10] A better agreement with the radioactive data is, in fact, obtained if the exponential dependence is replaced for large ΔZ by a simple power law dependence, $\sigma_\alpha/\sigma_p=a\Delta Z^b$. In the following, such a dependence is assumed for ΔZ larger than $Z_i/2$, which is the limit of our measurements. Parameters a and b are determined to assure continuity of both σ_α/σ_p values and derivatives with that computed from formula (9).

Comparisons of the Fe, O, and C fragmentation data from this work to the empirical formula are shown in Figs. 4 (left-hand side) and 5. The empirical predictions are also compared in Figs. 6 and 7 to existing isotopic cross section σ_α/σ_p ratios for Ni, Fe, Si, and Mg fragmentation at 1.15 and 0.70 GeV/nucleon, for Al fragmentation at 0.23 GeV/nucleon, and for O and C fragmentation at 1.15, 0.70, and 0.23 GeV/nucleon. Very good agreement is found in all cases, except for the σ_α/σ_p(Fe$\rightarrow^{22}$Na) at 700 MeV/nucleon measured by Raisbeck and Yiou.[10] However, we note that in this last case σ_α/σ_p(Fe$\rightarrow^{22}$Na) is unexpectedly greater than σ_α/σ_p(Fe$\rightarrow^7$Be), perhaps indicating larger errors than are assumed. Although this empirical fit was derived from the charge changing cross section systematics, the

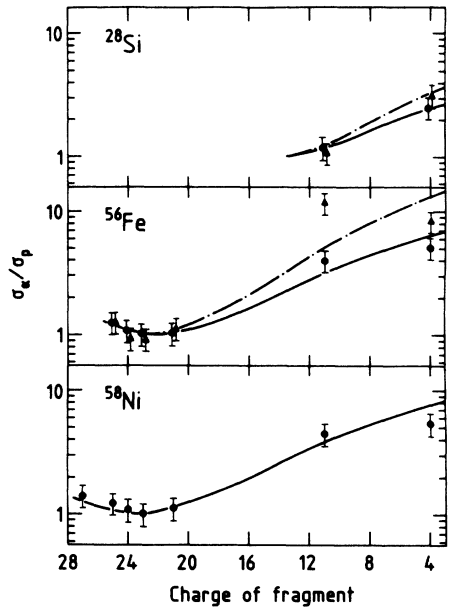

FIG. 6. Comparison of isotopic cross sections σ_α/σ_p ratios measurements for fragmentation of Ni, Fe, and Si, with the empirical formula discussed in text. Data points are from Raisbeck and Yiou (Ref. 10), at 0.70 GeV/nucleon (filled triangles), and 1.15 GeV/nucleon (filled circles). No error were reported for the data, but 20% of the uncertainty is assumed to be representative as suggested in the work of Raisbeck and Yiou. When cross section results were given for several isotopes of the same element (Co and Mn fragments), an average σ_α/σ_p ratio is computed from the sum of the isotopic cross sections. The solid lines are the empirical formula results at 1.15 GeV/nucleon, the dashed-dotted lines at 0.70 GeV/nucleon.

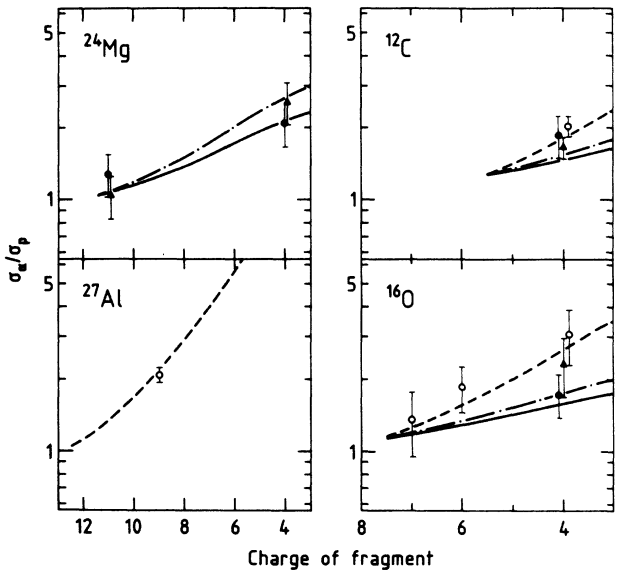

FIG. 7. Same as in Fig. 6, for Al, Mg, O, and C fragmentation. Data are isotopic cross sections measurements from Ref. 10 for Mg, O, and C at 1.15 GeV/nucleon (filled circles) and 0.70 GeV/nucleon (filled triangles), and from Ref. 22 for Al, O, and C at 0.23 GeV/nucleon (open circles). Solid lines are empirical formula results at 1.15 GeV/nucleon, dashed-dotted lines at 0.70 GeV/nucleon, and dotted lines at 0.23 GeV/nucleon.

good agreement with the isotopic cross section data suggests that isotopic effects should not be too important as far as the σ_α/σ_p ratios are concerned, and in the limit of the still large uncertainties of available isotopic measurements.

VI. APPLICATION TO COSMIC-RAY TRANSPORT

The most widely used model of propagation of cosmic rays is the leaky-box model.[3] In this steady state and homogeneous model, the primary cosmic rays emitted by cosmic-ray sources suffer inelastic collisions during their propagation in the interstellar medium (ISM), giving rise to secondary cosmic rays. Moreover, primary and secondary nuclei escape the galaxy, and are decelerated via ionization energy losses. The escape from the galaxy is characterized by the path length distribution of cosmic rays, which in the leaky-box model is an exponential of average Λ_{esc}. Λ_{esc} is usually expressed in g/cm^2 of interstellar material. The steady state equation for the interstellar flux J_i of a given cosmic-ray isotope i is

$$J_i(1/\Lambda_d+1/\Lambda_{esc})+\partial/\partial E\,[(dE/dx)_i J_i] = Q_i+\sum_k J_k/\Lambda_{ki}\ , \quad (10)$$

where Λ_d is the destruction length of the isotope i in the ISM, Q_i is the source strength for isotope i, J_k is the interstellar cosmic-ray flux of isotope k, Λ_{ki} is the characteristic length for isotope k to fragment into isotope i, and $(dE/dx)_i$ is the energy loss per g/cm^2 suffered by the isotope i. When compared to accurate cosmic-ray data, and using cross sections that were available in 1985, this simple model encounters some difficulties in simultaneously accounting for the B/C and Sc–Mn/Fe secondary/primary ratios, the Sc–Mn/Fe ratio being underestimated by about 10% when Λ_{esc} is derived from the B/C ratio.[5] The underprediction of Sc–Mn/Fe relative to B/C is very dependent on the whole set of σ_p, including those for B production. Actually, an important decrease in the Sc–Mn/Fe underprediction is expected when the recent semiempirical formulae of Webber[19] are used. The discussion of this point is, however, far beyond the scope of this work, and is relegated to a later paper. Here, we specifically focus on the differential effect between the predictions of the B/C and Sc–Mn/Fe ratios due to the presence of helium in the ISM, when compared to propagation calculations in pure hydrogen ISM. The magnitude of this effect is, in fact, independent of the σ_p used, and we have adopted the same set of hydrogen cross sections as used by the Saclay group.[5]

There exists numerous determinations of the galactic He/H ratio that are somewhat larger than the value 6.8% (by number) quoted by Cameron.[23] In main sequence B stars He/H is ~ 0.11,[24] in solar quiescent prominences He/H is 0.100 ± 0.025,[25] and in galactic ionization state H II regions He/H is ~ 0.11 according to Shaver.[26] In the following we assume an ISM helium fraction He/H of 0.10 for propagation calculations, in agreement with all these measurements.

The propagation code has been previously described

by Ferrando and Soutoul.[27] It is based on matrix formulation,[28] improved in order to take energy losses accurately into account. It was checked against a more standard propagation code (weighted-slab technique), and both codes were found to give similar results within better than 1% down to interstellar energies of ~300 MeV/nucleon. It treats all long-lived isotopes from ^{6}Li to ^{58}Ni. Total and partial cross sections in helium are introduced according to the empirical formulation described in the preceding section. The ionization energy losses in the ISM are computed as the weighted average of the energy losses in hydrogen and helium. Decay of ^{10}Be, ^{26}Al, ^{36}Cl, and ^{54}Mn is also taken into account, and the solar modulation is computed using the "force field solution"[29] parametrized by the deceleration potential ϕ. Computed B/C and Sc–Mn/Fe ratios are shown in Fig. 8 in both cases of pure hydrogen ISM and an ISM helium fraction He/H of 0.10, together with the satellite data of the IMP-8 and HEA03-C2 experiments,[6,1] and the latest balloon data of Webber *et al.*[30] In both cases, Λ_{esc} was adjusted in order that propagation results fit the B/C ratios measured in the HEA03-C2 experiment. The Λ_{esc} dependencies that were found to fit the data are (i) in pure hydrogen,

$$\Lambda_{esc}=24\times\beta\times R^{-0.65} \quad \text{for } R>5.5 \text{ GV},$$

$$\Lambda_{esc}=24\times\beta\times(5.5)^{-0.65} \quad \text{for } R<5.5 \text{ GV},$$

and (ii) with He/H=0.10,

$$\Lambda_{esc}=30.6\times\beta\times R^{-0.65} \quad \text{for } R>5.5 \text{ GV},$$

$$\Lambda_{esc}=30.6\times\beta\times(5.5)^{-0.65} \quad \text{for } R<5.5 \text{ GV},$$

β being the velocity of cosmic rays relative to the speed of light and R the rigidity. Propagation in an ISM including helium is seen to differ from propagation without helium in two points: First, the Λ_{esc} value necessary to fit the B/C ratio is increased and, second, the Sc–Mn/Fe ratio is lower with helium when B/C is accounted for. These two points are discussed in detail below.

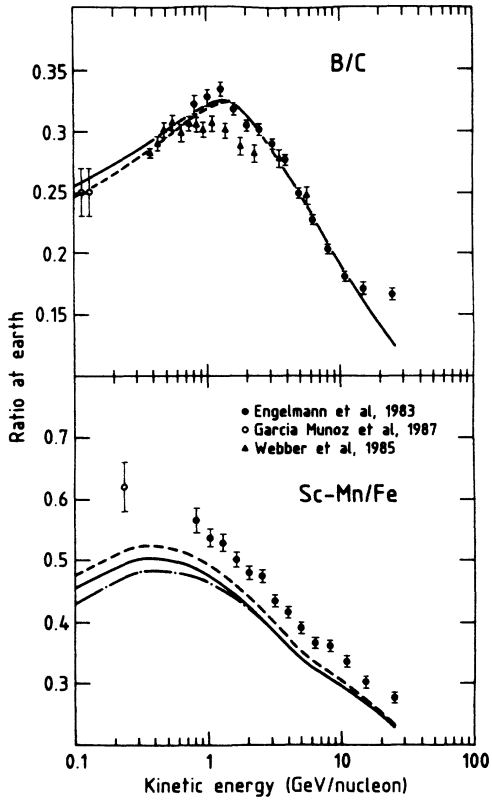

FIG. 8. Comparison of the measured B/C and Sc–Mn/Fe ratios with calculations in the leaky-box model, in the three cases of (i) pure hydrogen ISM (dashed line), (ii) He/H=0.10 in the ISM (solid line), and (iii) He/H=0.10 and assuming same energy losses in helium and hydrogen (dashed-dotted line, indistinguishable from the dashed line for the B/C ratio). Solar modulation is included, with $\phi=600$ MV for energies greater than 0.80 GeV/nucleon, and $\phi=490$ MV for lower energies. The Λ_{esc} dependence is given in the text. It was adjusted to fit the B/C ratio measured in HEA03-C2.

The Λ_{esc} values at 1 GeV/nucleon corresponding to the propagated curves of Fig. 8 are 7.2 g/cm^2 in the case of no helium and 9.2 g/cm^2 in the case of He/H=0.10. This Λ_{esc} increase is due to the longer "creation length" for B production, and to the larger (creation length)/(destruction length) ratio for B nuclei in helium, when referred to hydrogen. This can be clearly identified by considering the propagation of a unique primary P and a unique secondary S, and neglecting energy losses. With Λ_d the destruction length of the secondary, and Λ_{PS} the characteristic length for the primary to fragment into the secondary, the secondary/primary ratio S/P is given by

$$S/P=1/(\Lambda_{PS}/\Lambda_{esc}+\Lambda_{PS}/\Lambda_d) . \tag{11}$$

When referred to their values in a pure hydrogen medium, Λ_{PS} and Λ_{PS}/Λ_d are multiplied by factors $(1+4y)/(1+y\Gamma_{par})$ and $(1+y\Gamma_{tot})/(1+y\Gamma_{par})$, respectively, Γ_{par} and Γ_{tot} being the σ_α/σ_p ratio of partial and total cross sections, respectively, and with $y\equiv$He/H. Since both multiplying factors are greater than 1, it follows from (11) that Λ_{esc} must increase to fit a constant S/P ratio. In the case of the B/C ratio, Λ_d is roughly equal to Λ_{esc}, and both right-hand terms in (11) have the same order of magnitude. The increase of escape length (by a factor 1.28) is therefore mainly due to the increase of Λ_{PS} by the factor $(1+4y)/(1+y\Gamma_{par})=1.23$ for $\Gamma_{par}=1.4$, the increase of Λ_{PS}/Λ_d by a factor 1.04 playing a negligible role.

Turning now to the Sc–Mn/Fe ratio, it is seen in Fig. 8 that taking into account interstellar helium leads to an underprediction of Sc–Mn/Fe relative to pure hydrogen ISM, when B/C is equally accounted for. The Sc–Mn/Fe ratio is lowered by 5% up to ~1 GeV/nucleon, and by a smaller factor at higher energies (3% at 5 GeV/nucleon, less than 2% above 10 GeV/nucleon). The reason of this differential effect between B/C and Sc–Mn/Fe may be understood from the simplified expression (11). Contrary to the B/C ratio, the Sc–Mn/Fe ratio is dominated by the Λ_{PS}/Λ_d term, because Λ_d is about 3 times smaller than Λ_{esc}. Therefore, even when Λ_{esc} is increased to fit B/C (cancelling

almost all the effect of the increase of Λ_{PS} for Sc–Mn), the large difference in the σ_α/σ_p ratios for total and partial cross sections leads to an underprediction of Sc–Mn/Fe.

It is also worth noting that this differential effect due to cross sections is balanced at low energy for about one-half by the smaller energy losses per g/cm^2 in helium. This is illustrated in Fig. 8, which shows propagation results performed by considering equal energy losses in helium and hydrogen (dashed-dotted line).

Finally, interstellar helium is not expected to play a significant role regarding cosmic-ray isotopic anomalies and the B/C vs ^{15}N/O discrepancy.[31,32] Using our empirical formulation, no important differences were found with and without interstellar helium in the isotopic composition of Ne, Mg, and Si, and in the ^{15}N/O ratio. Although there may be departures of the systematics of σ_α/σ_p ratios for isotopic cross sections from that for charge changing cross sections, it seems unlikely that they can reach the high levels necessary to yield significant effects. For example, an increase of the propagated ^{15}N/O ratio by 10% would roughly require the ^{15}N production from oxygen in helium to be 2.5 times that in hydrogen, because of the low He/H interstellar ratio.

VII. CONCLUSIONS

The measurements presented here provide the first almost complete set of cross sections for C + α, O+α, and Fe+α reactions at high energy. When compared to p-induced reaction cross sections, two main features have appeared: (i) the independence from energy of the σ_α/σ_p ratio for total cross sections, and (ii) the increase of the σ_α/σ_p ratio of partial cross sections with the charge change, this increase being strongly dependent on the energy. From these measurements, we have derived an empirical formula for the σ_α/σ_p ratios that was found to generally agree with available isotopic cross sections ratios as well. Taking into account spallation of cosmic rays against interstellar helium, it was shown that the prediction of the Sc–Mn/Fe ratio in the standard leaky-box model is decreased by about 5% relative to the B/C ratio. This systematic effect is larger than the accuracy achieved now in the measurements of cross sections and cosmic-ray ratios. It must therefore be taken into account when addressing specific propagation questions such that of a possible truncation of path lengths.

ACKNOWLEDGMENTS

It is pleasure to thank C. Blondel and R. Roques-salane for their important contribution to the building of the ^{4}He target. We also are grateful for the considerable help from the entire staff at Lawrence Berkely Laboratory, especially from H. Crawford and J. Engelage. One of us (P.F.) is greatly indebted to J. P. Meyer for many valuable discussions.

[1] J. J. Engelman, P. Goret, E. Juliusson, L. Koch-Miramond, P. Masse, A. Soutoul, B. Byrnak, N. Lund, B. Peters, I. L. Rasmussen, M. Rotenberg, N. J. Westergaard, in Proceedings of the 18th International Cosmic Ray Conference, Bangalore, 1983, Vol. 2, p. 17.

[2] W. R. Weber, in *Workshop on Cosmic Ray and High Energy Gamma Ray Experiments for the Space Station Era, 1985,* edited by W. V. Jones and J. P. Wefel (Center for Continuing Education, Baton Rouge, 1985), p. 283.

[3] R. Cowsik, Y. Pal, S. N. Tandon, and R. P. Verma, Phys. Rev. **158**, 1238 (1967).

[4] J. A. Lezniak and W. R. Webber, Astrophys. Space Sci. **63**, 35 (1979).

[5] A. Soutoul, J. J. Engelmann, P. Ferrando, L. Koch-Miramond, P. Masse, and W. R. Webber, in Proceedings of the 19th International Cosmic Ray Conference, La Jolla, 1985, Vol. 2, p. 8.

[6] M. Garcia-Munoz, J. A. Simpson, T. G. Guzik, J. P. Wefel, and S. H. Margolis, Astrophys. J. Suppl. **64**, 269 (1987).

[7] P. Ferrando, P. Goret, and A. Soutoul, in Proceedings of the 19th International Cosmic Ray Conference, La Jolla, 1985, Vol. 3, p. 61.

[8] S. M. Read and V. E. Viola, At. Data Nucl. Data Tables **31**, 359 (1984).

[9] G. M. Raisbeck and F. Yiou, Phys. Rev. Lett. **35**, 155 (1975).

[10] G. M. Raisbeck and F. Yiou, in Proceedings of the 14th International Cosmic Ray Conference, Munich, 1975, Vol. 2, p. 506.

[11] W. R. Webber and D. A. Brautigam, Astrophys. J. **260**, 894 (1982).

[12] W. R. Webber, D. A. Brautigam, J. C. Kish, and D. A. Schrier, in Proceedings of the 18th International Cosmic Ray Conference, Bangalore, 1983, Vol. 2, p. 202.

[13] W. R. Webber and J. C. Kish, in Proceedings of the 19th International Cosmic Ray Conference, La Jolla, 1985, Vol. 3, p. 87.

[14] D. E. Greiner, P. J. Lindstrom, H. H. Heckman, B. Cork, and F. S. Bieser, Phys. Rev. Lett. **35**, 152 (1975).

[15] H. H. Heckman, D. E. Greiner, P. J. Lindstrom, and F. S. Bieser, Phys. Rev. Lett. **28**, 926 (1972).

[16] P. J. Lindstrom, D. E. Greiner, H. H. Heckman, B. Cork, and F. S. Bieser, Lawrence Berkeley Laboratory Report LBL-3650, 1975.

[17] H. C. Bradt and B. Peters, Phys. Rev. **77**, 54 (1950).

[18] G. D. Westfall, L. W. Wilson, P. J. Lindstrom, H. J. Crawford, D. E. Greiner, and H. H. Heckman, Phys. Rev. C **19**, 1309 (1979).

[19] W. R. Webber, in Proceedings of the 20th International Cosmic Ray Conference, Moscow, 1987, Vol. 2, p. 463.

[20] J. Jaros, A. Wagner, L. Anderson, O. Chamberlain, R. Z. Fuzesy, J. Gallup, W. Gorn, L. Schroeder, S. Shannon, G. Shapiro, and H. Steiner, Phys. Rev. C **18**, 2273 (1978).

[21] J. R. Radin, H. Quechon, G. M. Raisbeck, and F. Yiou, Phys. Rev. C **26**, 2565 (1982).

[22] J. R. Radin, A. R. Smith, and N. Little, Phys. Rev. C **9**, 1718 (1974).

[23] A. W. C. Cameron, in *Essays in Nuclear Astrophysics,* edited by C. Barnes, D. Clayton, and D. Schramm (Cambridge Uni-

versity, London, 1982), p. 23.
[24]S. C. Wolff and J. N. Heasley, Astrophys. J. **292**, 589 (1985).
[25]J. N. Heasley and R. W. Milkey, Astrophys. J. **221**, 677 (1978).
[26]P. A. Shaver, in Proceedings of the ESO Workshop on Primordial Helium, Garching, 1983, edited by P. A. Shaver, D. Kunth, and K. Kjar, p. 299.
[27]P. Ferrando and A. Soutoul, in Proceedings of the 20th International Cosmic Ray Conference, Moscow, 1987, Vol. 2, p. 231.
[28]R. Cowsik and L. W. Wilson, in Proceedings of the 13th International Cosmic Ray Conference, Denver, 1973, Vol. 1, p. 500.
[29]L. J. Gleeson and W. I. Axford, Astrophys. J. **154**, 1011 (1968).
[30]W. R. Webber, J. C. Kish, and D. A. Schrier, in Proceedings of the 19th International Cosmic Ray Conference, La Jolla, 1985, Vol. 2, p. 16.
[31]J. P. Meyer, in Proceedings of the 19th International Cosmic Ray Conference, La Jolla, 1985, Vol. 9, p. 141.
[32]W. R. Webber and M. Gupta, in Proceedings of the 20th International Cosmic Ray Conference, Moscow, 1987, Vol. 2, p. 129.

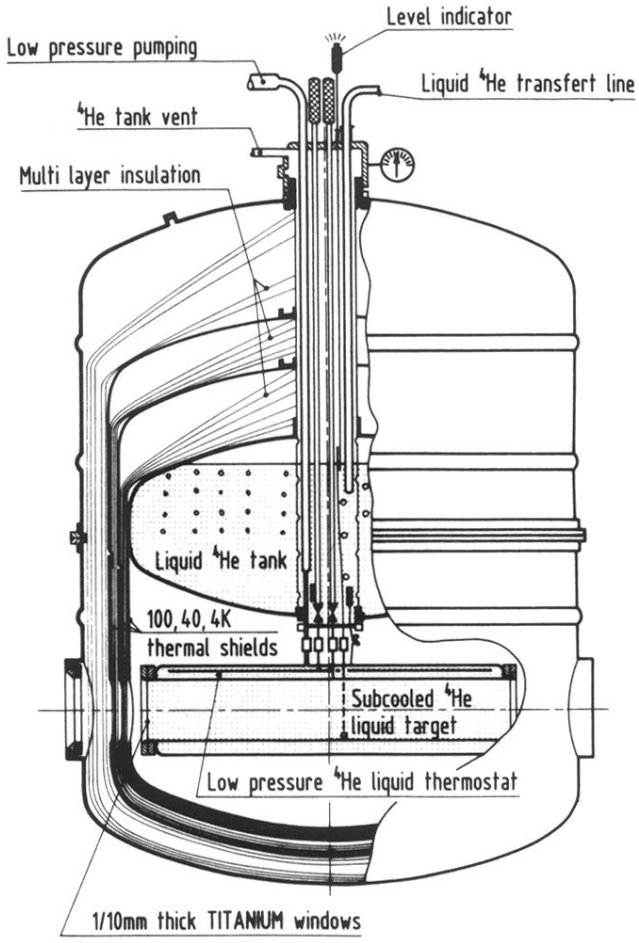

FIG. 2. Sketch of the liquid helium target.